SRTTU

JCARME
ISSN: 2228-7922
Journal of Computational and Applied Research in Mechanical Engineering
Vol. 9, No. 2, pp. 199-210
jcarme.sru.ac.ir

Automatic implementation of a new recovery coefficient for reliable contour milling

E. Bahloul* **and C. Rebiai**

Mechanical Engineering Department, Faculty of Technology, Batna 2 University, Fesdis-05000, Batna, Algeria

Article info:
Type: Research
Received: 09/01/2018
Revised: 18/10/2018
Accepted: 20/10/2018
Online: 22/10/2018

Keywords:
Cutting parameter,
Reliable trajectory,
Optimized overlap,
Automatic implementation.

Abstract
In contour milling, to render the machining process more automated with significant productivity without remaining material after machining, a new recovery coefficient was developed. The coefficient was inserted in the computation of contour parallel tool paths to fix the radial depth of cut in the way to ensure an optimized overlap area between the passes in the corners, without residuals. Thus, this parameter, which has been earlier inserted by the user, is now being independent and is implemented automatically from the input data of the contour shape of the pocket. In order to prove the effectiveness of the present approach, a detailed comparison with the classical methods found in the literature we also performed. The results clearly show that the new method removes the residuals efficiently in an automatic way and minimizes the toolpath length respect to the other methods. Furthermore, this proposed approach can easily be worked on the actual machine tool.

Nomenclature

L_{ij}	(mm)	j^{th} segment length of i^{th} contour
L_{oj}	(mm)	j^{th} segment length of pocket limit
R	(mm)	radius of tool
ρ_{opt}	——	optimized recovery coefficient
P_{ass}	(mm)	total length of passage lines
d_r	(mm)	radial depth of cut
T_{cal}	(min)	calculated milling time
Vf	(m/min)	feed rate
Vr	(rpm)	rotational speed
nd	——	number of discontinuities in one outline
n	——	number of contour
N	——	number of edges in one contour
e	(mm)	finishing thickness
r_j	(mm)	radius of the connecting arc between edges
N	——	number of edges in one contour
e	(mm)	finishing thickness
r_j	(mm)	radius of the connecting arc between edges

1. Introduction

Rough machining in CNC machine tool is a crucial parameter for machining efficiency, which has been enhanced in several directions [1-3]. To improve productivity in pocket milling,

* *Corresponding author*
email address: elhachemibahloul@yahoo.fr

a lot of research works oeuvres have been realized to improve the machining methods [4-8]. Optimization of machining paths is influenced by three factors, in particular; the choice of the machining strategy, the optimization of the remains material after machining and minimizing users maneuver in the aim to render the process more automated.

Concerning the choice of the machining strategy, there are two trajectory types of recess pocket. The first one uses the pocket boundary as a reference to form the parallel contours, and it is called “Trajectory by Contour parallel offset” (CPO) [9]. The second one uses an exceptional direction, and it is calculated by using the “Zigzag paths” method [10]. In this last type, the parallel segments are joined with other ones in opposition in such a way that orders the tool to slow down. In addition, with this strategy, it is essential to do finishing toolpath in all pocket contour boundaries to remove the residual and obtain the preferred shape. It is very difficult to achieve this additional finishing toolpath when the limits of the pocket have a complex shape [11, 12]. Contrariwise with the CPO toolpaths, the limits of the pocket shape are used to generate the principal offset contours. However, the offset contours are joined with them by a passage segment of the tool [13]. The number of discontinuities is less than that of Zigzag paths, thereby providing less time in the pocket milling. Moreover, there are three classical methods of calculation to generate the CPO toolpaths; Voronoï Diagram [14, 15], Pair Wise Offset [16] and Pixel Based Method [17, 18]. In this family of toolpaths, another mode is formed called spiral contours [19].

Generally, the sum of the length of each contour and the pass segment between the contours give the total length of the machining path. The comparing works for the machining strategies made in the literature prove that in most cases the contour parallel offset CPO toolpath are best suited due to their optimal trajectory generation compared with the Zigzag paths strategy [20]. On the other side, the whole length of toolpath can be optimized by decreasing the number of contours. This requires growing radial depth of cut. However, in this time, when the interval between contours increases, the probability of appearance of remaining material after machining between passes in the corners increases (Fig. 1(a)) [21]. Moreover, the report tool/work surface enables the occurrence of residuals in the center of the pocket (Fig. 1(b)) [13]. In the present work, a solution for efficient machining with CPO toolpaths without residuals is proposed. In addition, a new recovery coefficient, inserted in the computation of contour parallel tool paths that, in the first purpose, improves the machining in terms of no machined regions and of computing times compared to the others approach, is proposed.

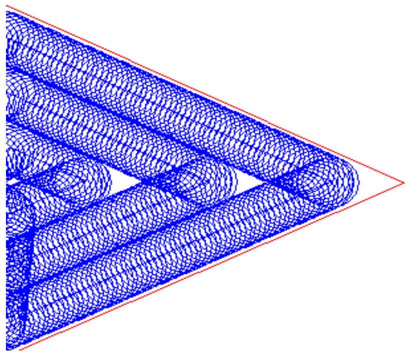

(a)

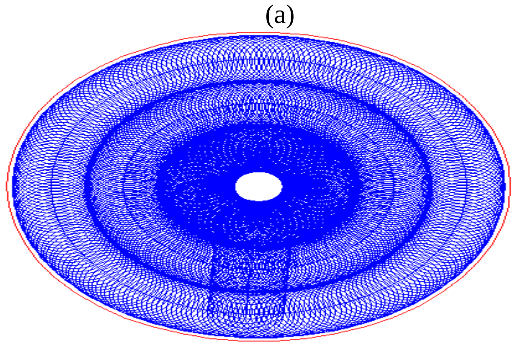

(b)

Fig. 1. No machined regions representation; (a) between passes, and (b) in the center of the pocket.

2. Related works

Significant attention has been ported to the optimization in contour parallel milling [22-24], especially the optimization of no machined regions which has received so much attention.

2.1. Uncut regions optimization

In the aim to eliminate the no machined regions in all angles of CPO and which are related to the large distance between the passes, Park et al. [13, 25] developed an algorithm (Pair-Wise Interference Detection) that detects the no machined area and add a supplementary path to remove them (Fig. 2(a)). However, these appended loops oblige the tool to slow down at each change of direction witch penalizes the total milling time. Mansor et al. [26] added a small segment to each discontinuity in order to eliminate the no machined area; this method causes the tool to do a back and forth with the same disadvantage (Fig. 2(b)). Choy and Chan [27] developed an application in the software Unigraphics (UG) Version 17.0 suggesting a single loop or double loops of toolpath in each angle of CPO in order to remove the residual completely (Fig. 2(c)).

The optimization of non-machined areas has the purpose of choosing the best removal method that reduces more the cutting time. Among the effective approaches in this domain, and which are inserted into computers-aided manufacturing software, Cimatron E9.0, Mastercam X, and Power MILL 10.0 (Fig. 3) are distinguished.

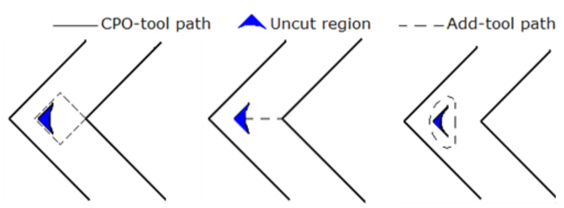

(a) (b) (c)

Fig. 2. Removal methods for the no machined area; (a) PWID loop, (b) compensation segment, and (c) reduced loop.

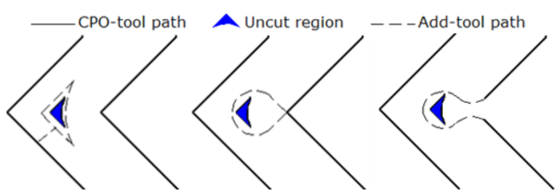

(a) (b) (c)

Fig. 3. Machining of uncut regions with effective CAM software; (a) Cimatron, (b) Mastercam, and (c) Power- mill**.**

In the heart of the recent works made in the literature, Zhao et al. [28] and Zhou et al. [29] used a toolpath loop to eliminate completely and efficiently the no machined residual without tool retractions, where the size of the no machined region is detected (Fig. 4), using the following formula.

$$U = \left(\left(R - 2R * overlap \right) \Big/ \sin \frac{\alpha}{2} \right) - R \tag{1}$$

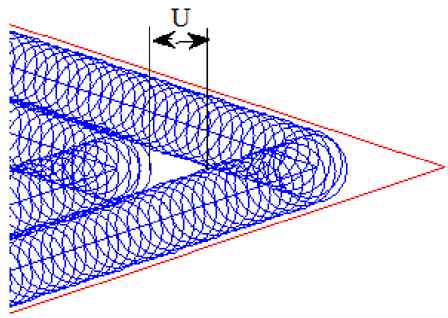

Fig. 4. Uncut region size.

The residual material is the area, which appears when $U > 0$ (Fig. 5), and the size of the additional loop is as follow [28]:

$$L_{loop} = 2P + L_{arc} = (2R)^2 \left\{ \begin{array}{l} \left(\frac{1}{2} - \text{overlap} \right)^2 \text{cog} \frac{\alpha}{2} - \left(\frac{1}{2} - \text{overlap} \right) \sqrt{\text{overlap} - \text{overlap}^2} - \\ \frac{1}{1440} \left[180 - \alpha - 2 \arccos \left(1 - 2\text{overlap} \right) \right] \end{array} \right\} \tag{2}$$

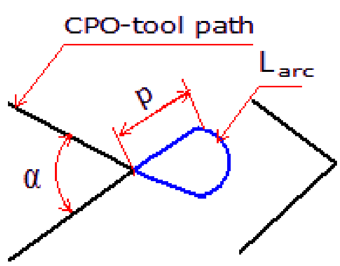

Fig. 5. Representation of the appended loop.

Lin et al. [30] located the no machined areas by the analysation of the all pocket surface to be machined and appended an additional toolpath through the bisectors of the pocket shape. The tool on one bisector must cross a length $L_{bisector}$ computed as in Fig. 6 by:

$$L_{bisector} = \left(L_{oj} * \sin \frac{\alpha_{(j-1)}}{2} \Big/ \sin \left(\pi - \frac{\left(\alpha_j + \alpha_{(j-1)} \right)}{2} \right) \right) - \left(R + e \right) \Big/ \sin \frac{\alpha_j}{2} \tag{3}$$

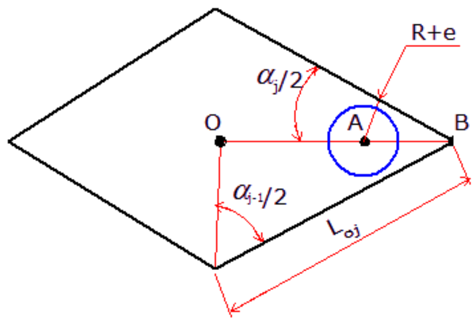

Fig. 6. Toolpath on a bisector.

Among the latest works in the optimization of no machined area, the present authors developed a method called "LOM" [31], where the recovery coefficient ensures an overlap area in all corners of the pocket except the smallest one, where there is no an overlap area and no uncuts. This may cause a residual in this angle, especially when the feed rate increases. So, where the pocket includes several small and equal angles, it is necessary to add a few toolpaths in order to have a smooth surface without residual material on the surface. For these reasons, another coefficient is proposed in the following which will be more generalized and ensure an optimized overlap area between the passes in all cases.

3. Optimized overlap area without uncut regions.

3.1. CPO toolpath generation

In the first section, the realization of the parallel contours is seen to depend primarily on the shape of the pocket limits. Consequently, an algorithm is proposed to describe any arbitrary form of pocket limit concave or convex with segment-segment or segment - arc at first. Then, a second algorithm gives the CPO tool paths. Through the parameters of the pocket shape (lengths L_{oj}, arcs r_j and angles between edges α_j) the shape of the pocket boundary can be determined by their vertices point P_j. The algorithm that reflects the outside contour of the pocket is presented in Appendix A.

The essentials to form the contour parallel toolpaths, are the use of the bisectors of all corners as intersection points of each pair of segments and join them with arcs. Then, the passage of an offset contour to another is delivered by a passage segment throughout the corner bisector of the pocket form Fig. 7.

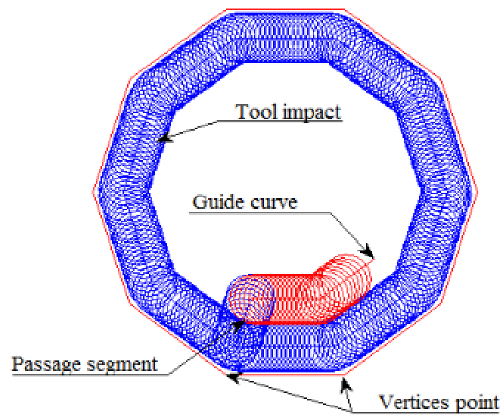

Fig. 7. CPO toolpath representation.

The full length (L_{ip}) of the CPO toolpaths in the inner part is the total toolpath length (L_{ij} and $L_{arc(ij)}$) of each contour and the sum of the passage segment (P_{ass}) between contours as given in Eqs. (4, 5 and 7). The algorithm that reflects the CPO toolpaths is presented in Appendix B.

The radial depth of cut ($d_r = 2R*(1-overlap)$) is fixed by the passage segment between passes as given in the following formula, and it may be inserted by the user. In the aim to ensure an overlap area between the passes in the corners, the recovery coefficient $(1-overlap)$ must be taken between 0 and 1.

$$L_{ip} = \sum_{i=1}^{n}\sum_{j=1}^{N}\left(L_{ij} + L_{arc(ij)}\right) + P_{ass} \tag{4}$$

with:

$$L_{arc(ij)} = r_{arc(ij)} * (\pi - \alpha_j) \tag{5}$$

$$P_i = \frac{2R*(1-overlap)}{\sin\left(\alpha_{\min}^{i}/2\right)} \tag{6}$$

$$P_{ass} = \sum_{i=1}^{n-1} P_i \tag{7}$$

3.2. Optimized recovery coefficient

In the contour parallel milling, it is very difficult to ensure a coverage zone between the passes to eliminate any kind of residual, because the distance between passes should not protrude the diameter of the cutter. For this, it is necessary to find a recovery coefficient (ρ) which will be multiplied by the diameter in order to remove this residual. This coefficient must be inserted in the calculation of the offset contours.
In the previous work [31], the recovery coefficient ensures an overlap area in all corners of the pocket except the smallest one, where there is no overlap area and no uncut (Fig. 8(a)). This may cause a residual in this angle, especially if the feed rate increases. Then, it is necessary to define a new recovery coefficient (ρ_{opt}) from the smallest angle in the aim to ensure a minimum coverage zone in all corners where the smallest angle is found (See Eq. (8)), Fig. 8(b)). Several tests are performed for any radius of the tool ranging up to 100 mm with this new recovery coefficient. It is found that for many angles values $(0 < \alpha < \pi)$ the overlap area between passes in corner for the smallest angle of the pocket is much optimized according to Table 1. In addition, a detailed comparison of the coefficients is carried out in Table 2.

$$\rho_{opt} = \left((R-1)\sin\frac{\alpha_{j(\min)}}{2} \Big/ 2R \right) + 0.5 \tag{8}$$

According to Table 1, the good news is that the overlap area between the passes in the smallest angle increase proportionally with the tool radius. On the other hand, for Table 2, it is clearly legible that the new coefficient is always small of that where there is no overlap and no unmachined area. Therefore, an optimized overlap area is ensured between the passes in the corner of the smallest angle.
To better optimize the CPO toolpath length, where the pocket shape includes just one smallest angle, the overlap coefficient must be calculated from the second smallest angle, because the toolpath length increases where the angle becomes small. So the residual in the first one will be removed by the passage segment of the tool between contours. This novel optimized recovery coefficient may is noted to be applicable to any shape of pocket contour automatically.

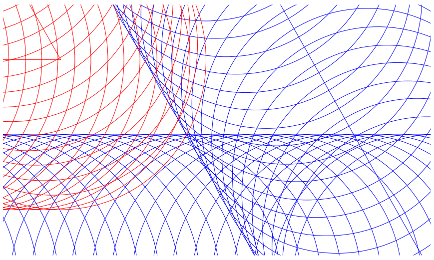

(a)

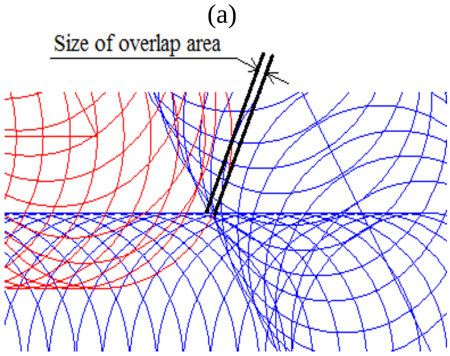

(b)

Fig. 8. Machining simulation at the smallest angle; (a) without overlap area using “LOM” [31], and (b) with an optimized overlap area using “ ρ_{opt} ”.

4. Implementation

The main program that uses several algorithms, including those expressed in this article, has been realized in MATLAB code. These algorithms have been amply examined for several pocket shapes with machining simulation of the trajectory of the tool. For this main program, the input data are the edges length L_{oj}, arcs r_j, and angles α_j between edges for the pocket form. The number m, the radii R_i, the number of teeth Z_i, the feed per tooth $fz_{(i)}$ for each set of tools are available on the machine and the cutting speed V_c for the combination (tool/part/machine).

Table 1. Size of overlap area for several values of the smallest angle according to the radius of tool.

Angle (°)	10	30	50	70	90	110	130	150	170
Overlap area (mm) with:									
R=5 mm	0.09	0.26	0.42	0.57	0.71	0.82	0.91	0.96	1.00
R=10 mm	0.08	0.26	0.42	0.56	0.70	0.82	0.92	0.96	1.00
R=20 mm	0.08	0.28	0.44	0.56	0.72	0.80	0.92	0.96	1.00
R=30 mm	0.06	0.24	0.42	0.54	0.72	0.84	0.90	0.96	1.02
R=40 mm	0.08	0.24	0.40	0.56	0.72	0.80	0.96	0.96	1.04
R=50 mm	0.10	0.30	0.40	0.50	0.70	0.80	0.90	0.90	1.00

Table 2. Coefficients comparison.

Angle (°)	10	30	50	70	90	110	130	150	170
Recovery coeff-(LOM) [28]	0.543	0.629	0.711	0.786	0.853	0.909	0.953	0.982	0.998
New recovery coefficient with:									
R=5 mm	0.534	0.603	0.669	0.729	0.782	0.827	0.862	0.886	0.898
R=10 mm	0.539	0.616	0.690	0.758	0.818	0.868	0.907	0.934	0.948
R=20 mm	0.541	0.622	0.700	0.772	0.835	0.889	0.930	0.958	0.973
R=30 mm	0.542	0.625	0.704	0.777	0.841	0.895	0.938	0.966	0.981
R=40 mm	0.542	0.626	0.706	0.779	0.844	0.899	0.941	0.970	0.985
R=50mm	0.542	0.626	0.707	0.781	0.846	0.901	0.944	0.973	0.988

For the outputs, the program gives a value of the optimized recovery coefficient (ρ_{opt}), the coordinates of each segment of contour offset (x_i, y_i- x_f, y_f), toolpath length with the associated milling time, and machining simulation (guide curve and tool effect). In the aim to prove the effectiveness of the present method, respect to the others in terms of optimization of no machined area and milling time, the following example is suggested. Where the shape of the pocket surface representing the worst choice for the present approach; it is the form having acute angles (Fig. 9).

Since the new recovery coefficient is calculated through the smallest angle and if this last one is acute, the radial depth of cut reduces; therefore, the trajectory of the tool becomes longer, consequently with more discontinuities, and the tool must decelerate in each one, which penalizes the present approach. For this, the total time (τ_{tot}= 0.177s) is used in the calculation (calculated cutting time, Eq. (9) Banerjee et al. [22]), which is necessary for the starting acceleration and the final deceleration. This value is injected into the calculation because in the present approach there are more contours, which mean more discontinuities respect to the other methods.

The cutting conditions are those used by Ramaswami et al. [32], where the milling speed is selected as 36.6 m/min, and the rapid feed rate is underneath 36 m/min.

$$T_{cal} = \sum_{i=1}^{n}\sum_{j=1}^{N}\left(\frac{L_{ij}}{V_f}\right) + 2*(1+nd)*\tau_{tot} \tag{9}$$

The machining simulation shows that the CPO toolpaths in the present approach are more numerous (Fig. 10). But the addition of supplementary paths with other methods rends the trajectory of the tool longer than that of the present approach in most cases.

The results shown in Table 3 indicates that the present method is more effective compared to the other approaches on a large set of tool (five and six of the eight valid tools for the comparison to machine the entire pocket). Table 3 also illustrates that from the radius (R=10 mm), the tool moves with the same path length in all methods. It should be noted that generally, the angles of the CPO are not acute, and then the suggested method becomes more efficient in term of cutting time respect to the classical approaches.

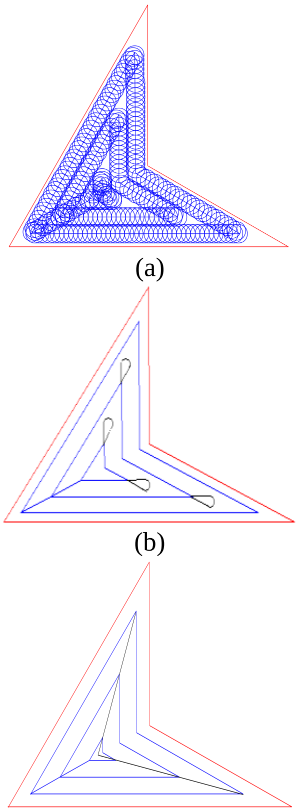

Fig. 9. Machining simulation with tool radius R=4 mm and ρ = 0.9; (a) without appended toolpath, (b) Zhao additional loop, and (c) Lin appended bisector segment.

The other methods [28-30] use a recovery coefficient up or equal to 0.9 to reduce the number of CPO; consequently, the tool path length decreases too. According to Table 2, when the value of the angle decreases the new recovery coefficient decreases too, for example (α=30°, ρ=0.6), (α=90°, ρ= 0.8). This difference between 0.6 and 0.9 or 0.8 and 0.9 means that the radial depth with ρ=0.6 is smallest to that of ρ= 0.8; therefore, there are more contours using the small coefficient. It can be said that with an acute angle, there is more contours respect to the other methods using a recovery coefficient near to 1. From another standpoint, as seen in Table 2, the recovery coefficient decreases when the radius of the tool becomes small, and he present approach is also less effective than the other methods. For these reasons, the present method is not efficient with the tool of radius 2 and 3 mm (Table 2).

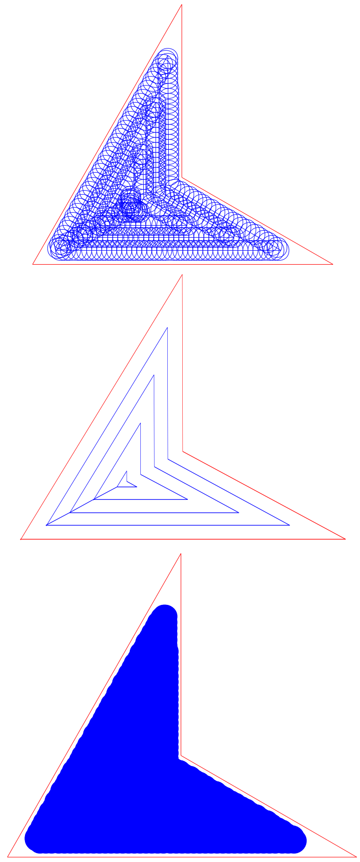

Fig. 10. Machining simulation with our method, tool radius R=4 mm and ρ_{opt} = 0.5970.

Table 3. Comparison of cutting methods

Tool radius (mm)	Present method (min)	Lin method [30] (min)	Zhao [28] (min)
2	19.51	17.23	15.46
3	15.15	14.97	13.25
4	08.49	09.30	08.21
5	05.34	06.17	05.51
6	04.16	04.42	04.69
7	03.29	03.83	04.37
8	02.70	03.74	04.61
9	02.14	03.49	04.76
10	02.03	02.03	02.03
13	01.14	01.14	01.14
20.46	00.00	00.00	00.00

It should also be noted that if the angles of the pocket limits become no acute, the present method becomes more effective with the use of all tools. It is worth noting that, the calculation of the CPO toolpath lengths with Zhao and Lin method is performed according to Eqs. (1, 2 and 3).

5. Conversion of the program into machine language

To perform the conversion of the program into machine language, it is sufficient to transmit the segments coordinates of the offset contours directly to the machine tool from the result file as illustrated in the following example (Fig. 11(b)) where the coordinates of each segment (x_i, y_i and x_f, y_f) of CPO toolpaths are given by the program after injection of new recovery coefficient. Then, the G01 function is applied to all segments; the result is an efficient machining with an optimized toolpath length without uncut regions (Fig. 12). For this example, it is noted that the input data are: an equilateral triangle with a length edge equal to 100 mm and the tool radius equal to 8 mm.

As introduced at first, for a recovery coefficient equal to 0.9, the result of the machining shows that an abandoned residual appears in the center of the part as well as in the angles of CPO toolpaths (Fig. 12(a)). Thereafter, the new recovery coefficient is injected. Then, the result file (Figure 11(b)), that represents the coordinates of the CPO tool paths (x_i, y_i and x_f, y_f of each segment), is transferred directly to the machine tool. The result of the real experiment is perfect machining without any residual either between the passes or in the peripheral of the pocket (Fig. 12(b)).

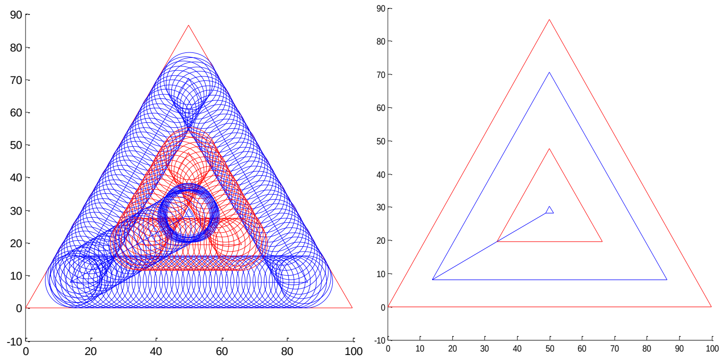

(a)

```
seg =                                        seg =                                        seg =

   13.8564    8.0000   86.1435    8.0000        33.7736   19.4992   66.2263   19.4992        48.7115   28.1236   51.2884   28.1236

seg =                                        seg =                                        seg =

   86.1435    8.0000   50.0000   70.6025        66.2263   19.4992   50.0000   47.6041        51.2884   28.1236   50.0000   30.3553

seg =                                        seg =                                        seg =

   50.0000   70.6025   13.8564    8.0000        50.0000   47.6041   33.7736   19.4992        50.0000   30.3553   48.7115   28.1236

ro =                                          ro =

    0.7187                                        0.7187

pass =                                       pass =

   13.8564    8.0000   33.7736   19.4992        33.7736   19.4992   48.7115   28.1236

LcontL =

    362.1977

fx >>
```

(b)

Fig. 11. Result file; (a) Machining simulation with guide curve and tool impact, and (b) Coordinates of contours segments and total toolpath length Lcontlwith ρ_{opt} = 0.7187.

(a)

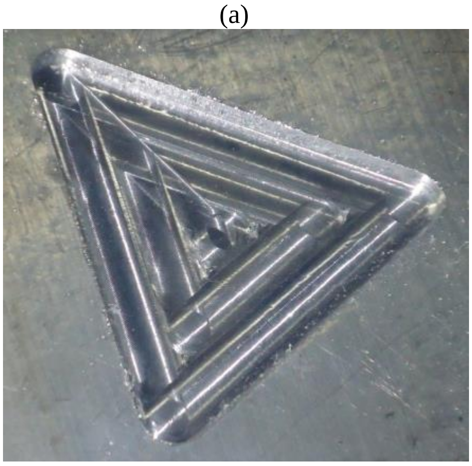

(b)

Fig. 12. Real machining; (a) a residual material with ρ = 0.9, and (b) perfect machining without residual material ρ_{opt} = 0.7187.

6. Conclusions

The problem typically encountered in machining area is the no machined regions left by tool. This study proposes a new recovery coefficient in the calculation of CPO toolpath. This developed coefficient is found to be numerically and experimentally more efficient than other methods and ensures a minimum overlap between passes in order to fix the radial depth of cut. This new recovery coefficient has also given a longer lifetime of the tool since its interval between contours is smaller respect to that of the other methods, and it can be inserted automatically. It is clearly revealed that the proposed coefficient improves significantly the cutting efficiency.

Appendix

Appendix A

The algorithm that reflects the pocket limits is:
// Input: length of segments, L_{oj}, α_j, r_j
// Output: pocket limits with { L_{oj}, $L_{arc(oj)}$, p_j}
Begin
{If $j=1$:

$$P(j,1) = x_0, P(j+1,1) = x_0 + L_{01}$$

$$P(j,2) = y_0, P(j+1,2) = y_0$$

$$L_{arc(0j)} = r_j * (\pi - \alpha_j)$$

$$angle = \pi$$

(The first edge with two vertex point and arc)
Else if $j=2: N$

$$P(j+1,1) = P(j,1) \pm L_{0j} * \cos(angle)$$

$$P(j+1,2) = P(j,2) \pm L_{0j} * \sin(angle)$$

$$L_{arc(o(j+1))} = r_{(j+1)} * (\pi - \alpha_{(j+1)})$$

$$angle = angle + \alpha_{(j-1)} - \pi$$

(The other vertices point with edges and arcs)}
End

Appendix B

The algorithm that describes the CPO tool paths.

// Input: pocket limits with,{L_{oj}, $L_{arc(oj)}$, P_j}
// Output: generation of CPO toolpaths{L_{ij}, $L_{arc(ij)}$, n}
Begin
S: Number of segments that will disappear.
Calcul of the recovery coefficient with Eq. (8).
Calcul of the passage segment P_{ass} with Eqs. (6 and 7).
For $i==1:n$
$J==1:N$

$$L_{arc(ij)} = r_{arc(ij)} * (\pi - \alpha_j)$$

{If: $L_{arc(oj)} > 0$

$$L_{arc((i+1)j)} = (r_{arc(ij)} - F) * (\pi - \alpha_j) \text{ and } L_{(i+1)j} = L_{ij}$$

Else :

$$L_{(i+1)j} = L_{ij} + \left(r_{arc(ij)} * \cot\left(\frac{\alpha_j}{2}\right)\right) - F * \left(\cot\left(\frac{\alpha_j}{2}\right) + \cot\left(\frac{\alpha_{(j+1)}}{2}\right)\right)$$

End}

{If: $L_{ij}^{s} \leq 0$, the (s+1) angles become a single one:

$$\alpha_{(j+1)} = \left(\alpha_j^1 + ... + \alpha_j^s + \alpha_j^{(s+1)}\right) - s * \pi$$

The two segments which delimit those who have disappeared $L_{(i+1)j}$, $L_{(i+1)(j+1)}$, becomes:

$$L_{(i+1)j} = L_{ij} - F * \cot\left(\frac{\alpha_{(j+1)}}{2}\right) + L_{i(j+1)}^{s} * \sin\left(\pi - \gamma_2\right) / \sin\left(\alpha_{(j+1)}\right)$$

$$L_{(i+1)(j+1)} = L_{i(j+s+1)} - F * \cot\left(\frac{\alpha_{(j+1)}}{2}\right) + L_{i(j+1)}^{s} * \sin\left(\pi - \gamma_1\right) / \sin\left(\alpha_{(j+1)}\right)$$

and N decreases to N-S

End

$L_p = L_{ij} + X_t$ }

End

(For the first contour: $i = 1 \rightarrow F = R+e$ else: $F = 2R*(1\text{-}overlap)$)

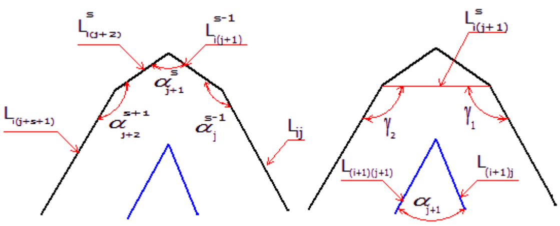

Fig. 13. CPO toolpaths when some segments disappear.

Acknowledgements

This work is supported by the post-graduation of the Mechanical Department, Faculty of Technology of the University of Batna 2, Algeria.

References

[1] H. b. Liang, Y Z. Wang, and X. LI,"Implementation of an adaptive feed speed 3D NURBS interpolation algorithm", *Front. Mech. Eng*, Vol. 1, No. 4, pp. 403−408, (2006).

[2] R. QI, W. Liu, H. Bian, and L. Li,"Five-axis rough machining for impellers", *Front. Mech. Eng*, Vol. 4, No. 1, pp.71-76, (2009).

[3] F. Monies, I. Danis, C. Bes, S. Cafieri, andM.Mongeau, "A new machining strategy for roughing deep pockets of magnesium-rare earth alloys", *Int J. Adv. Manuf. Technol*,Vol. 92, No. 9-12, pp. 3883-3901, (2017).

[4] T. Fu, J. Zhao, and W. Liu,"Multi-objective optimization of cutting parameters in high-speed milling based on grey relational analysis coupled with principal component analysis", *Front. Mech. Eng*, Vol. 7, No. 4, pp.445-452, (2012).

[5] C. K. Hyun, G. L. Sung, andY. Y.Min,"An optimized contour parallel tool path for 2D milling with flat end mill", *Int J. Adv. Manuf. Technol*, Vol. 31, No. 5, pp.567-573, (2006).

[6] M. Dotcheva, K. Dotchev, and I. Popov, "Modeling and optimization of up and down milling processes for a representative pocket feature", *Int J. prec. Eng Manuf*, Vol. 14, No. 5, pp.703-708, (2013).

[7] F. Y. Han, D. H. Zhang, M. Luo,and B. H. Wu, "Optimal CNC plunge cutter selection and tool path generation for multi-axis roughing free-form surface impeller channel", *Int J. Adv. Manuf. Technol*, Vol. 71, No. 9, pp.1801-1810, (2014).

[8] S. Sui, Y. Li, W. Shao, and P. Feng, "Tool path generation and optimization method for pocket flank milling of aircraft structural parts based on the constraints of cutting force and dynamic characteristics of machine tools", *Int J. Adv. Manuf. Technol*, Vol. 85, No. 5-8, pp. 1553-1564, (2016).

[9] S. C. Parc, and Y. C. Chung, "Offset tool-path linking for pocket machining", *Computer Aided Design*, Vol. 34, No. 4, pp. 299-308, (2002).

[10] S. C. Park, and B. K. Choi, "Tool-path planning for direction-parallel area milling", *Computer Aided Design*, Vol. 32, No. 1, pp.17-25, (2000).

[11] C. Göloglu, and Y.Arslan, “Zigzag machining surface roughness modeling using evolutionary approach”, *J Intell. Manuf*, Vol. 20, No. 2, pp. 203-210, (2009).

[12] P. Selvaraj, and P. Radhakrishnan, “Algorithm for Pocket Milling using Zig-zag Tool Path”, *Defence Science Journal*, Vol. 56, No. 2, pp.117-127, (2006).

[13] S. C. Park,and B. K. Choi, “Uncut free pocketing tool-paths generation using pair-wise offset algorithm”, *Computer Aided Des*, Vol. 33, No. 10, pp.739-746, (2001).

[14] M. Held,“ Voronoi diagrams and offset curves of curvilinear polygons”, *Computer Aided Design*, Vol. 30, No. 4, pp. 287-300,(1998).

[15] R. Ramamurthy, and R. T.Farouki,“ Voronoi diagram and medial axis algorithm for planar domains with curved boundaries”, *Journal of Computational and Applied Mathematics*, Vol. 102, No. 1, pp. 253-277, (1999).

[16] B. K. Choi, S. C. Park, “A pair-wise offset algorithm for 2D point-sequence curve”, *Computer Aided Design*, Vol. 31, No. 12, pp.735-745,(1999).

[17] B. K. Choi, B. H. Kim,“Die-cavity pocketing via cutting simulation”, *Computer Aided Design*, Vol. 29, No. 12, pp. 837-846, (1997).

[18] C. K. Hyun, “Tool path modification for optimized pocket milling”, *International Journal of Production Research*, Vol. 45, No. 24, pp.5715-5729, (2007).

[19] A. Banerjee, H. Y. Feng, andE. V.Bordatchev,“ Process planning for Floor machining of 2½D pockets based on a morphed spiral tool path pattern”, *Computers and Industrial Engineering*, Vol. 63, No. 4, pp. 971-979, (2012).

[20] A. Abdullahil,“Selection of efficient cut pattern in simple pocket machining”, *International Conference on Mechanical Engineering*, Dhaka, Bangladesh, AM, , Vol. 79, pp. 1-6, (2007).

[21] M. Held, G. Lukacs, and L. Andor, “Pocket machining based on contour parallel tool paths generation by means of proximity maps”, *Computer Aided Design*, Vol. 26, No. 3, pp.189-203, (1994).

[22] S. Sui, Y. Li, W. Shao, and P. Feng, “Tool path generation and optimization method for pocket flank milling of aircraft structural parts based on the constraints of cutting force and dynamic characteristics of machine tools”, *Int J. Adv. Manuf. Technol*, Vol. 85, No. 5-8, pp. 1553-1564, (2016).

[23] F. Monies, I. Danis, C. Bes, S. Cafieri, and M. Mongeau, “A new machining strategy for roughing deep pockets of magnesium-rare earth alloys”, *International Journal of Advanced Manufacturing Technology*, Vol. 92, No. 9-12, pp. 3883-3901, (2017).

[24] F. Y. Han, D. H. Zhang, M. Luo, and B. H. Wu,“Optimal CNC plunge cutter selection and toolpath generation for multi-axis roughing free-form surface impeller channel”, *International Journal of Advanced Manufacturing Technology*, Vol. 71, No. 9-12, pp. 1801-1810, (2014).

[25] S. C. Park, Y. C. Chungb, and B. K. Choi,“ Contour parallel offset machining without tool-retractions”, *Computer Aided Design*, Vol. 35, No. 9, pp.841-849, (2003).

[26] M. S. A. Mansor, S. Hinduja, and O. Owodunni,“ Voronoi diagram-based tool path compensations for removing uncut material in 2½D pocket machining”, *Computer Aided Design*, Vol. 38, No. 3, pp. 194-209, (2006).

[27] H. S. Choy, and K. W.Chan,“A corner-looping based tool path for pocket milling”, *Computer Aided Design*, Vol. 35, No. 2, pp.155-166, (2003).

[28] Z. Y. Zhao, C. Y. Wang, H. M. Zhou, Z. Qin, “Pocketing toolpath optimization for sharp corners”, *Journal of Materials Processing Technology*, Vol. 192, No. 193, pp.175-180, (2007).

[29] M. Zhou, G. Zheng, and S. Chen,“ Identification and looping tool path generation for removing residual areas left by pocket roughing”, *Int. J. Adv.*

Manuf. Technol, Vol. 87, No. 1-4, pp. 765-778, (2016).

[30] Z. Lin, J Fu, H. Shen, and W. Gan, "Global Uncut Regions Removal for Efficient Contour-Parallel Milling", *International Journal of Advanced Manufacturing Technology*, Vol. 68, No. 5, pp. 1241–1252, (2013).

[31] E. Bahloul, M. Brioua, and C. Rebiai, "An efficient contour parallel tool path generation for arbitrary pocket shape without uncut regions", *International Journal of Precision Engineering and Manufacturing*, Vol. 16, No. 6, pp.1157-1169, (2015).

[32] H. Ramaswami, R. S. Shaw, and S. Anand, "Selection of optimal set of cutting tools for machining of polygonal pockets with islands", *Int J. Adv. Manuf. Technol*, Vol. 53, No. 9, pp.963–977, (2011).

How to cite this paper:

E. Bahloul and C. Rebiai, "Automatic implementation of a new recovery coefficient for reliable contour milling", *Journal of Computational and Applied Research in Mechanical Engineering*, Vol. 9, No. 2, pp. 199-210, (2019).

DOI: 10.22061/jcarme.2018.3225.1360

URL: http://jcarme.sru.ac.ir/?_action=showPDF&article=889